An Autofocus Method for SAR Frequency-Domain Backprojection Imaging

Liming Zhou, Xiaoling Zhang, Jun Shi, Shunjun Wei, Jing Ming, Liang Li, Yangyang Wang
School of Information and Communication Engineering, University of Electronic Science and Technology of China
Chengdu, P. R. China
Email: limingzhou_cd@foxmail.com

***Abstract*—Frequency-Domain Backprojection Algorithm (FDBP) is a new imaging method which is more efficient than Time-Domain Backprojection Algorithm (TDBP) and also can be applied to arbitrary aperture geometry. And autofocus method is a vital technology for high-precision Synthetic Aperture Radar (SAR) imaging, especially for Airborne SAR. However, traditional autofocus methods usually suffer from heavy computation burden or compensate partly, and there are no special autofocus methods for FDBP. In this paper, a novel fast autofocus method is proposed for FDBP to compensate phase error in wavenumber domain by estimating motion error. The estimated error of Antenna Phase Centers (APCs) can be applied to imaging achieving the spectrum compensation for the whole scene. The motion error is estimated based on the optimal criterion of maximum image sharpness. The expression of APC error estimation is derived and Conjugate Gradient (CG) is utilized to solve the optimization problem. The simulation and experimental examples verify the validity of the proposed method.**

Keywords—Synthetic Aperture Radar(SAR), Frequency-Domain Backprojection Algorithm (FDBP), autofocus imaging, maximum sharpness, High-precision motion compensation

I. INTRODUCTION

Many imaging algorithms have been developed for high-resolution and efficient SAR imaging. Those algorithms for SAR are mainly divided into two categories such as frequency domain algorithms and time domain algorithms. The widely used frequency domain algorithms are Range Doppler (RD) [1], Chirp Scaling (CS) [2] and Wavenumber Domain (Omega-K, ωK) [3]. The frequency domain algorithms need to approximate the echo mode, which causes the deterioration of image quality image. The typical time domain imaging algorithm is the Time Domain Back Projection (TDBP), which has the advantages of high precision compensation of curve wave-front effect and adjusting to a variety of complex flight paths. However, TDBP algorithm suffers from heavy computation burden due to calculating the distance history between APC and pixels. Many new imaging algorithms based on BP algorithm have been proposed to improve the efficiency and accuracy of SAR imaging. Of the newly methods, Frequency Domain Back Projection (FDBP) has been considered an excellent one for high-resolution and high-efficiency imaging.

Same as TDBP algorithm, FDBP algorithm has the highly accurate compensation and is suitable for complex flight path. In addition, the advantage of the FDBP algorithm is that it can generate an arbitrary sampling of the SAR image spectrum [4] and is more efficient than TDBP algorithm [5]. However, it is also sensitive to the positions of antenna phase centers (APCs) which are effected by vibration of the carrier platform and the error of trajectory. Therefore motion compensation must be carefully considered in the FDBP imaging.

Since navigation data correction can't compensate the motion error precisely in the wavelength scale by Global Positioning System (GPS) and inertial measurement unit (IMU), it is necessary to use data driven autofocus techniques. Traditional autofocus methods based on phase error function such as Phase Gradient Autofocus, Map Drift and Phase Difference are not suitable for TDBP and FDBP. Autofocus algorithms based on radar imaging quality have been extensively studied, such as minimum entropy, maximum sharpness and maximum contrast.

Comparing with other metrics-based autofocus algorithms, optimize sharpness metrics can produce excellent restorations [6]. There are many autofocus algorithms based on optimize sharpness metrics recently. In [7], an autofocus approach based on maximizing image sharpness was proposed for TDBP, in which it demonstrates a natural geometric interpretation that allows for optimal single-pluse phase corrections to be derived in closed form as the solution of a quartic polynomial to reduce the burden of computation. But this method is still computationally intensive, because it needs all the values of backprojection to compute eigenvalue matrix. In [8], an autofocus method based on Maximum image sharpness for Fast Factorized Back-projection (FFBP) was proposed, which utilize coordinate descent optimization and secant method to obtain phase errors. In [9], an autofocus method based on maximum image sharpness was presented via semidefinite programming to estimate phase errors of the APCs. However the aim of these methods were to estimate the phase errors of each APCs, which can't satisfy all the pixels of the whole scene and is not suitable for the framework of FDBP. In [10], a motion compensation method for BP (named as TDBP-AF) based on maximum image intensity was proposed using part of the pixels to improve the computation efficiency. But the performance of this algorithm is not good when too few pixels are selected. And it also suffers from heavy computation efficiency for the whole scene.

In this paper, an autofocus method based on maximum image sharpness, named as FDBP-AF is proposed for FDBP to estimate motion errors. In the scheme, a model of estimating position error for FDBP, is established based on maximum image sharpness. Conjugate gradient method is used to obtain optimal estimate of motion error. Compared with other autofocus methods, it can figure out the motion error accurately to compensate phase error in wavenumber domain of the whole scene and has the advantage of higher efficiency on account of FDBP based SAR imaging rather than TDBP based. Moreover, in this paper, the algorithm calculates 2D coordinates for the compensation of 2D

spectrum, which is easier to apply to 3D SAR imaging by compensating 3D spectrum.

II. FDBP Imaging and Problem Formulation

A. Signal Model of FDBP

The geometry of SAR imaging with motion errors is illustrated in Fig.1. Suppose that Pe and Pr denote the error position of APC measured by GMS or IMU and the real position of APC respectively for each aperture. Let P denote the one point target in the imaging scene.

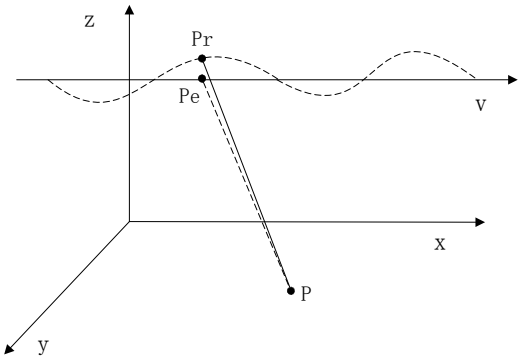

Fig. 1. The geometric model of SAR with motion errors.

FDBP is derived from TDBP, but the domains of the two projections are different. TDBP is the coherent accumulation of echoes after the range compression at different azimuth times in the time domain, and its general form [1] can be expressed as

$$h(\mathbf{\Phi}) = \int_t s(t,|r|)|r|\,dt \tag{1}$$

Where, t is the orientation moment, and $s(t,r)$ is the echoes after the range compression. $r=|\mathbf{\Phi}-\mathbf{\Phi}_t|$ denotes the distance between the position of APCs and scatters in the imaging scene. let $\mathbf{\Phi}_t=[x(t),y(t),z(t)]\in R^3$ denote the positions of APCs, $\mathbf{\Phi}=[x,y,z]\in R^3$ indicate the positions of the scene, which can be approximated to discrete cells in the scene.

Taking the multidimensional Fourier transform of (1) in the $\mathbf{\Phi}$ domain and making some transformation [1], general FDBP integral formulation can be expressed as

$$H(\mathbf{K}) = \int_t e^{-jK\mathbf{\Phi}_t}\hat{S}(t,|\mathbf{K}|)dt \tag{2}$$

Where $\hat{S}(t,|K|)$ is the Fourier transform of $\hat{s}(t,|\mathbf{K}|)$, and $\hat{s}(t,|\mathbf{K}|)=a(r)s(t,r)r$. $a(r)$ compensates the amplitude to construct Fourier transform instead of Hankel transform, whose effect on the amplitude of the final focused image is negligible. $\mathbf{K}$ is the wavenumber vector.

Finally, we can get the imagery in time domain by inverse Fourier transform. It is written as

$$h(\mathbf{\Phi}) = \int_{\mathbf{K}} H(\mathbf{K})e^{jK\mathbf{\Phi}}d\mathbf{K} \tag{3}$$

FDBP imaging requires three steps. Firstly, according to (2), the backprojection values of image spectrum are obtained from the spectrum of the raw echo for each aperture, and the phase compensation factor $e^{-j\mathbf{K}\mathbf{\Phi}_t}$ is multiplied. Then, the image spectrum of each aperture is accumulated to reconstruct the final image spectrum. Finally, the imagery in time domain can be calculated by the inverse Fourier transform of the image spectrum.

The imaging scheme of FDBP is similar to TDBP, except that the projected domain is different. The latter reconstructs the SAR image directly from the time-domain echo after range compression by coherent accumulation, while the former reconstructs the spectrum of the SAR image from the echo spectrum and obtain SAR image from image spectrum.

The efficiency of FDBP imaging is higher than TDBP. FDBP is not necessary to calculate the distance from each pixel of the scene to the antenna for each aperture. Instead, it only calculates the Index matrix at once. Because the backprojection distance $\mathbf{K}$ of the FDBP is independent on the position of the APC for each aperture. The values of matrix $\mathbf{K}$ are the same for each aperture. Moreover, in the imaging process the Fourier Transform and the inverse Fourier Transform can be replaced by a fast Fourier transform, which can improve the imaging efficiency.

B. Motion Errors

According to (2), it can be known that the imaging quality is related to the motion error of APC.

Let $\tilde{\mathbf{\Phi}}_t=[\tilde{x}(t),\tilde{y}(t),\tilde{z}(t)]\in R^3$ denote measurement position of APC, and $\Delta\mathbf{\Phi}_t=[\Delta x(t),\Delta y(t),\Delta z(t)]\in R^3$ denotes the motion error of APC at slow time t. In order to reduce the number of estimates, we can represent $\tilde{\mathbf{\Phi}}_t$ and $\Delta\mathbf{\Phi}_t$ again as $\tilde{\mathbf{\Phi}}_t=[\tilde{r}(t),\tilde{y}(t)]\in R^2$ and $\Delta\mathbf{\Phi}_t=[\Delta r(t),\Delta y(t)]\in R^2$ for 2-D imaging, which can improve the efficiency of the calculation and the accuracy of the estimation. Therefore, the spectral imaging corresponding to motion errors compensated by vector $\Delta\mathbf{\Phi}_t$ can be expressed as:

$$H(\mathbf{K};\Delta\mathbf{\Phi}_t) = \int_s e^{-j\mathbf{K}(\tilde{\mathbf{\Phi}}_t+\Delta\mathbf{\Phi}_t)}\hat{S}(t,|\mathbf{K}|)dt \tag{4}$$

The image in time domain after compensating motion error is written as

$$h(\Delta\mathbf{\Phi}_t) = \int_{\mathbf{K}} H(\mathbf{K};\Delta\mathbf{\Phi}_t)e^{jK\mathbf{\Phi}}d\mathbf{K} \tag{5}$$

Let $\Delta\hat{\mathbf{\Phi}}_t$ denote the estimate of $\Delta\mathbf{\Phi}_t$,which is the result of autofocus to optimize the image. In this paper, we choose the maximum sharpness as the evaluation metrics for focusing image. The model for estimating the motion error of APC via the maximum sharpness metrics can be expressed as follow

$$\Delta\hat{\mathbf{\Phi}}_t=\arg\max_{\Delta\hat{\mathbf{\Phi}}}\left\|h(\Delta\hat{\mathbf{\Phi}}_t)h^*(\Delta\hat{\mathbf{\Phi}}_t)\right\|_2^2 \tag{6}$$

III. FDBP Autofocus

The sharpness of the image can be expressed as

$$E(\Delta\hat{\mathbf{\Phi}}_t) = \int_{\mathbf{\Phi}}\left|g(\Delta\hat{\mathbf{\Phi}}_t)\right|^2 d\mathbf{\Phi} \tag{7}$$

Where, $g(\Delta\hat{\boldsymbol{\Phi}}_t)=h(\Delta\hat{\boldsymbol{\Phi}}_t)h^*(\Delta\hat{\boldsymbol{\Phi}}_t)$ is the image intensity. Combining (7), (6) can be rewritten as follow to estimate the motion errors of the APCs.

$$\Delta\hat{\boldsymbol{\Phi}}_t=\arg\max_{\Delta\boldsymbol{\Phi}_t}\left\{f_0(\Delta\hat{\boldsymbol{\Phi}}_t)\right\}=\arg\min_{\Delta\boldsymbol{\Phi}_t}\left\{f(\Delta\hat{\boldsymbol{\Phi}}_t)\right\} \quad (8)$$

Where, $f(\Delta\hat{\boldsymbol{\Phi}}_t)=-f_0(\Delta\hat{\boldsymbol{\Phi}}_t)$.

We use the CG method to solute the model. The partial derivative function of $f(\Delta\hat{\boldsymbol{\Phi}}_t)$ needs to be displayed, which can be expressed as

$$\begin{aligned}\frac{\partial f(\Delta\hat{\boldsymbol{\Phi}}_t)}{\partial\Delta\hat{\boldsymbol{\Phi}}_t}&=-2\sum_{\boldsymbol{\Phi}}\left|g(\Delta\hat{\boldsymbol{\Phi}}_t)\right|\frac{\partial g(\Delta\hat{\boldsymbol{\Phi}}_t)}{\partial\Delta\hat{\boldsymbol{\Phi}}_t}\\&=-2\sum_{\boldsymbol{\Phi}}\left|g(\Delta\hat{\boldsymbol{\Phi}}_t)\right|[h^*(\Delta\hat{\boldsymbol{\Phi}}_t)\frac{\partial h(\Delta\hat{\boldsymbol{\Phi}}_t)}{\partial\Delta\hat{\boldsymbol{\Phi}}_t}+h(\Delta\hat{\boldsymbol{\Phi}}_t)\frac{\partial h^*(\boldsymbol{\Phi};\Delta\hat{\boldsymbol{\Phi}}_t)}{\partial\Delta\hat{\boldsymbol{\Phi}}_t}]\\&=-4\sum_{\boldsymbol{\Phi}}\left|g(\Delta\hat{\boldsymbol{\Phi}}_t)\right|\mathrm{Re}\left[h^*(\Delta\hat{\boldsymbol{\Phi}}_t)\frac{\partial h(\Delta\hat{\boldsymbol{\Phi}}_t)}{\partial\Delta\hat{\boldsymbol{\Phi}}_t}\right]\end{aligned} \quad (9)$$

Where, the partial derivative of $h(\Delta\hat{\boldsymbol{\Phi}}_t)$ can be written as

$$\frac{\partial h(\Delta\hat{\boldsymbol{\Phi}}_t)}{\partial\Delta\hat{\boldsymbol{\Phi}}_t}=\int_{\mathbf{K}}\int_{t}e^{-j\mathbf{K}(\hat{\boldsymbol{\Phi}}_t+\Delta\hat{\boldsymbol{\Phi}}_t)}(-j\mathbf{K})\hat{M}(t,|\mathbf{K}|)\phi_2(\mathbf{K})dse^{j\mathbf{K}\boldsymbol{\Phi}}d\mathbf{K} \quad (10)$$

Line search is an important step for the CG method. In order to ensure that the value of the objective function is sufficiently reduced in the search direction, we used armijo line search method. Combined with the CG method, the steps of the motion errors estimation method are as follows

---

Step1: initialize $\Delta\hat{\boldsymbol{\Phi}}_t=\mathbf{0}$,iterative number N, calculate initial search direction $d_0=-\frac{\partial f(\Delta\hat{\boldsymbol{\Phi}}_t^0)}{\partial\Delta\hat{\boldsymbol{\Phi}}_t^0}$,let

$n=0$

While $n\le N$ **do**

Step2: using Armijo line search method to calculate step size λ_n,

$$f(\Delta\hat{\boldsymbol{\Phi}}_t^n+\lambda_n d_n)=\min f(\Delta\hat{\boldsymbol{\Phi}}_t^n+\lambda d_n)$$

Step3:estimate motion error $\Delta\hat{\boldsymbol{\Phi}}_t^{n+1}=\Delta\hat{\boldsymbol{\Phi}}_t^n+\lambda_n d_n$

$n\leftarrow n+1$

Step4: update search direction

$$d^{n+1}=-\frac{\partial f(\Delta\hat{\boldsymbol{\Phi}}_t^{n+1})}{\partial\Delta\hat{\boldsymbol{\Phi}}_t^{n+1}}+\beta^n d^n,$$

where $\beta^n=\dfrac{\left\|\frac{\partial f(\Delta\hat{\boldsymbol{\Phi}}_t^{n+1})}{\partial\Delta\hat{\boldsymbol{\Phi}}_t^{n+1}}\right\|^2}{\left\|\frac{\partial f(\Delta\hat{\boldsymbol{\Phi}}_t^{n})}{\partial\Delta\hat{\boldsymbol{\Phi}}_t^{n}}\right\|^2}$

End while

Compared with TDBP, FDBP only calculates the Index matrix at once , which is more efficient [5]. In the scheme of autofocus it can reduce the computation for each iteration. Moreover, since FDBP does not involve a Fourier transform along the aperture domain, parallel computing is available here. In our method we also exploit this feature to optimize the FDBP-AF algorithm.

IV. Result of Simulation and Experimental Data

A. Simulation Results

To demonstrate the effectiveness of FDBP autofocus method, the simulations are presented at first. The simulation parameters are shown in Tab. 1. Uniform random errors between $[-\frac{1}{4}\lambda,\frac{1}{4}\lambda]$ are added to the positions of APC in range dimension.

TABLE 1 Simulation Parameters

Parameters	value
Carrier Frequency	30 GHz
Time width	1us
Signal Bandwidth	300 MHz
Sampling Rata	390 MHZ
PRF	500 Hz
Platform Speed	50 m/s
Platform Height	4000 m
The APC Number	500

Fig.2 shows the imaging results of five points using a straight line as the inaccurate measuring positions of APCs, which are based on TDBP, TDBP-AF, FDBP and FDBP-AF, respectively. Fig.2(d) displays the imaging result using FDBP-AF, which demonstrates that the method is effective.

The computation platform is Inter I7-8700K 3.7GHz. FDBP-AF uses 1882s to obtain the motion error, whose size of image is 25×1000 and pixel spacing is 0.2m. TDBP-AF uses 5706s to estimate parameters, whose image size for autofocus is 25×25 in the scene center. The scene selected by TDBP-AF is smaller but it takes several times longer than FDBP-AF.

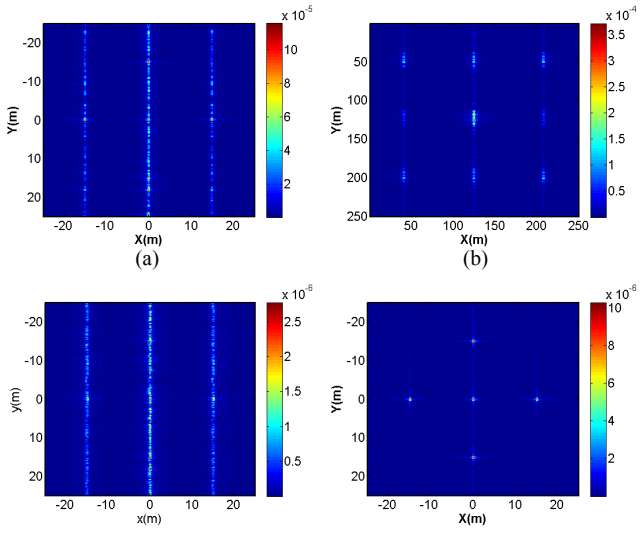

Fig. 2. The imaging results of the simulated point-targets. (a) TDBP without autofocus. (b) TDBP-AF. (c) FDBP without autofocus. (d) FDBP-AF.

In order to analyze the characteristics of the estimated motion errors of APCs, the estimated APC positions is compared with the real APC positions in the range direction and the azimuth direction. Fig. 3 shows that the APC positions estimated in the range direction can match the true APC positions, but there is a shifting in range direction and a few errors in azimuth direction. Although there is still an error in the azimuth and range directions, the point target is well focused. Because the estimate of the two directions jointly affect the imaging result in the continuous optimization of the image sharpness.

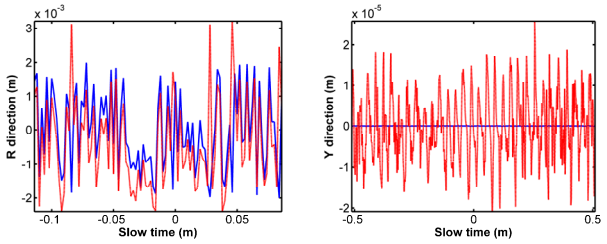

(a) (b)

Fig. 3. Comparision of estimated APC and actual APC. (a) Range-direction. (b) Azimuth direction

B. *Experimented Data*

The experimental LASAR raw data is implemented which was collected in an anechoic chamber. This system was designed for 3D-SAR imaging shown in Fig.4 (a), which can form a two-dimensional synthetic linear array. We only use some data collected from a horizontal (Y direction) motion trajectory of antenna to demonstrate the effectiveness of the autofocus method for 2D-SAR imaging. Moreover, this autofocus method can easily apply to 3D-FDBP imaging by extending the dimensions of the estimated parameters. The aim of this experiment is to demonstrate the effectiveness of the new method. The parameters of LASAR system are presented in Tab. 2.

TABLE 2 EXPERIMENTAL PARAMETERS

Parameters	value
Carrier Frequency	10GHz
Signal form	Steped frequency signal
Signal Bandwidth	2GHz
Sampling Rata	2GHZ
PRI	300ms
Platform Speed	50mm/s
The APC Number	85

The positions of the antenna was collected by software at equal time intervals assuming that the speed of antenna is constant. There is a uncertain movement error because of the non-uniform speed without a precision position measuring instrument. In order to exam the method proposed, uniform random errors between $[-\frac{1}{4}\lambda,\frac{1}{4}\lambda]$ are added to the positions of APCs in range direction. The targets consisted of two metallic spheres are shown in fig.4(b). The targets are placed 5 meters from the system.

Fig.5 indicates the imaging results of the two spheres using TDBP without autofocus, TDBP-AF, FDBP without autofocus and FDBP-AF, respectively. The average computational time of TDBP-AF is about 1031s, and the image size for TDBP-AF autofocus is 61×61 as shown in Fig5(a). It is failed to focus the image in this situation. In general, if the scene selected for autofocus is too small, the performance of TDBP-AF may be worse and even fail to focus. And it is hard to select more pixels for focusing because of the heavy computation burden increased greatly with the number of pixels. But the average computational time of motion error estimation of FDBP-AF is about 419s for the whole scene. The size of image for autofocus is 250×250 and pixel spacing is 0.02m. Notice that here we optimized the FDBP-AF algorithm by parallel computing because of its features of easy parallel programming to speed up the algorithm. The scene selected by TDBP-AF is smaller but it takes several times longer than FDBP-AF. So the result of focused image indicate the effectiveness of the FDBP-AF. And the comparison with TDBP-AF demonstrate that the performance of FDBP-AF is better.

(a) (b)

Fig. 4. The measurement setup. (a) LASAR system. (b) Photo of the two targets.

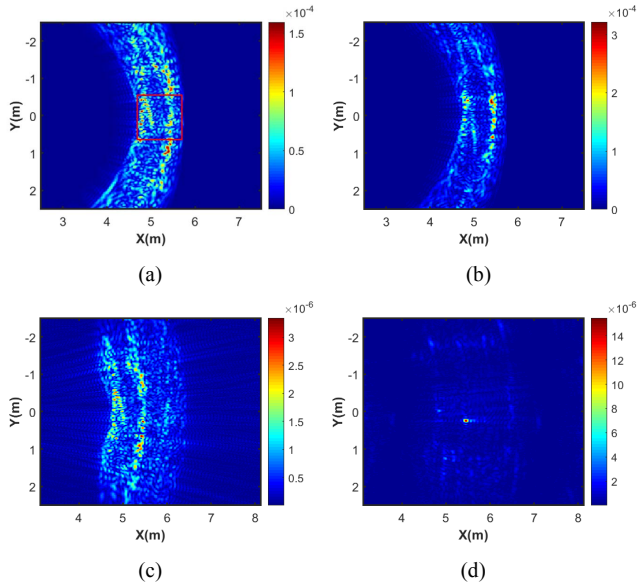

Fig. 5. The imaging results of the experimental two spheres. (a) TDBP without autofocus. (b) TDBP-AF. (c) FDBP without autofocus. (d) FDBP-AF.

V. CONCLUSIONS

In this paper, a new fast autofocus algorithm for FDBP is proposed to compensate phase error in wavenumber domain via optimization using the criterion of maximum image sharpness. The APCs error of two dimensions for motion error is estimated by using the conjugate gradient method,

which can be applied for the compensation of the whole scene. The parallel computing can be applied to FDBP to improve the efficiency. The results of simulation and experimental measurement confirm the effectiveness of the proposed method for autofocus imaging. Moreover, this method performs well and is more efficient than TDBP-AF.

ACKNOWLEDGMENT

This work was supported by the National Key R&D Program of China under Grant 2017YFB0502700, the National Natural Science Foundation of China under Grants 61671113, and 61571099, the Fund of High Level Academic Conference Program in the Graduate School of UESTC.

REFERENCES

[1] Bamler R, "A comparison of Range-Doppler and wavenumber domain SAR focusing algorithms," IEEE Transactions on Geoscience and Remote Sensing, pp. 706--713, 1992

[2] Raney, R. K, et al. "Precision SAR processing using chirp scaling."IEEE Transactions on Geoscience & Remote Sensing 32.4:786-799, 1994

[3] IReigber A, Alivizatos E, Potsis A, et al, "Extended wavenumber-domain synthetic aperture radar focusing with integrated motion compensation," in Radar, Sonar and Navigation, 153 Compendex, pp. 301--310, 2006.

[4] Zhe Li, Jian Wang, and Qing Huo Liu, "Frequency-Domain Backprojection Algorithm for Synthetic Aperture Radar Imaging." IEEE Geoscience and remote Sensing Letters 12.4:905-909, 2017

[5] L. Pu, X. Zhang, P. Yu and S. Wei, "A fast three-dimensional frequency-domain back projection imaging algorithm based on GPU," 2018 IEEE Radar Conference (RadarConf18), pp. 1173-1177, 2018.

[6] Morrison, R. L., M. N. Do, and D. C. Munson. "SAR image autofocus by sharpness optimization: a theoretical study." IEEE Transactions on Image Processing A Publication of the IEEE Signal Processing Society 16.9:2309, 2007

[7] Ash, Joshua N. "An Autofocus Method for Backprojection Imagery in Synthetic Aperture Radar." IEEE Geoscience & Remote Sensing Letters9.1:104-108, 2011.

[8] Li Y, Wu J, Pu W, et al. "An autofocus method based on maximum image sharpness for Fast Factorized Back-projection," IEEE Radar Conference, 1201-1204, 2017.

[9] Wei S J, Zhang X L, Hu K B, et al. "LASAR autofocus imaging using maximum sharpness back projection via semidefinite programming," IEEE Radar Conference, 1311-1315, 2015.

[10] Kebin, Hu , et al. "A High-precision Motion Compensation Method for SAR Based on Image Intensity Optimization." Journal of Radars, 4.1, 2015.